Table of Contents

Introduction and Experimental Overview

Valuable insights into nucleon and nuclear structure are possible when use is made of flavor degrees of freedom such as strangeness. The study of the electromagnetic production of strangeness using both nucleon and nuclear targets has proven to be a powerful tool to constrain QHD and QCD-inspired models of meson and baryon structure, and elastic and transition form factors [1-5].

By comparison, there are few experimental studies of charged weak transition form factors at intermediate energies [6-10]. With the new high-current, cw electron beam (CEBAF) at Jefferson Lab, it is now feasible to attempt a measurement of the weak production of strangeness to compliment the electromagnetic production data [11]. The reaction to be studied is:

$$\vec{e} + p \rightarrow \nu_e + \Lambda \qquad (1)$$

where $\vec{e}$ represents the incident (polarized) electron, p the proton target, ν is the electron neutrino, and Λ is the electroweakly-produced strange hyperon. The reaction proceeds via the exchange of the charged weak current as shown in Fig. 1. This reaction has never been observed before.

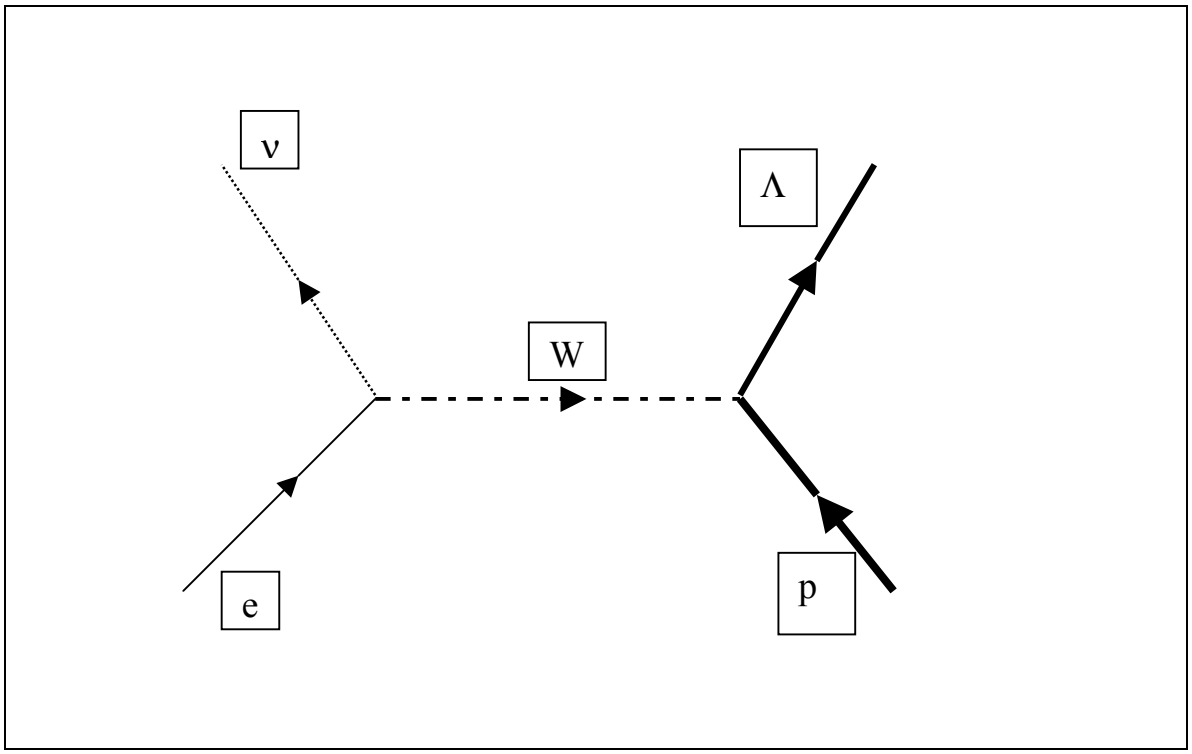

Fig. 1. The strangeness-changing weak charged-current reaction $\vec{e} + p \rightarrow \nu_e + \Lambda$. The neutrino in the reaction is not detected directly, but through its reconstructed missing mass once the Λ decay products are detected.

The Λ hyperon decays approximately 64% of the time into a proton and negative pion as shown in Fig. 2. The decay proton will be detected in the SOS while the negative pion from the decay will be detected in the Enge Split-pole Spectrometer as shown. The proton and pion information will be used to reconstruct the hyperon in the missing mass spectrum. Once the Λ-hyperon is identified in this way, its momentum and energy are determined. Then, using the information on the incident electron and the target proton, the neutrino is identified in a second missing mass calculation; the neutrino is not detected directly. Finally, the use of a polarized electron beam will facilitate the measurement using the neutrino's left-handedness; the electron neutrino will have its polarization vector opposite to the momentum vector. Only one electron helicity direction will produce the reaction (for a completely polarized beam) shown in Fig. 1.

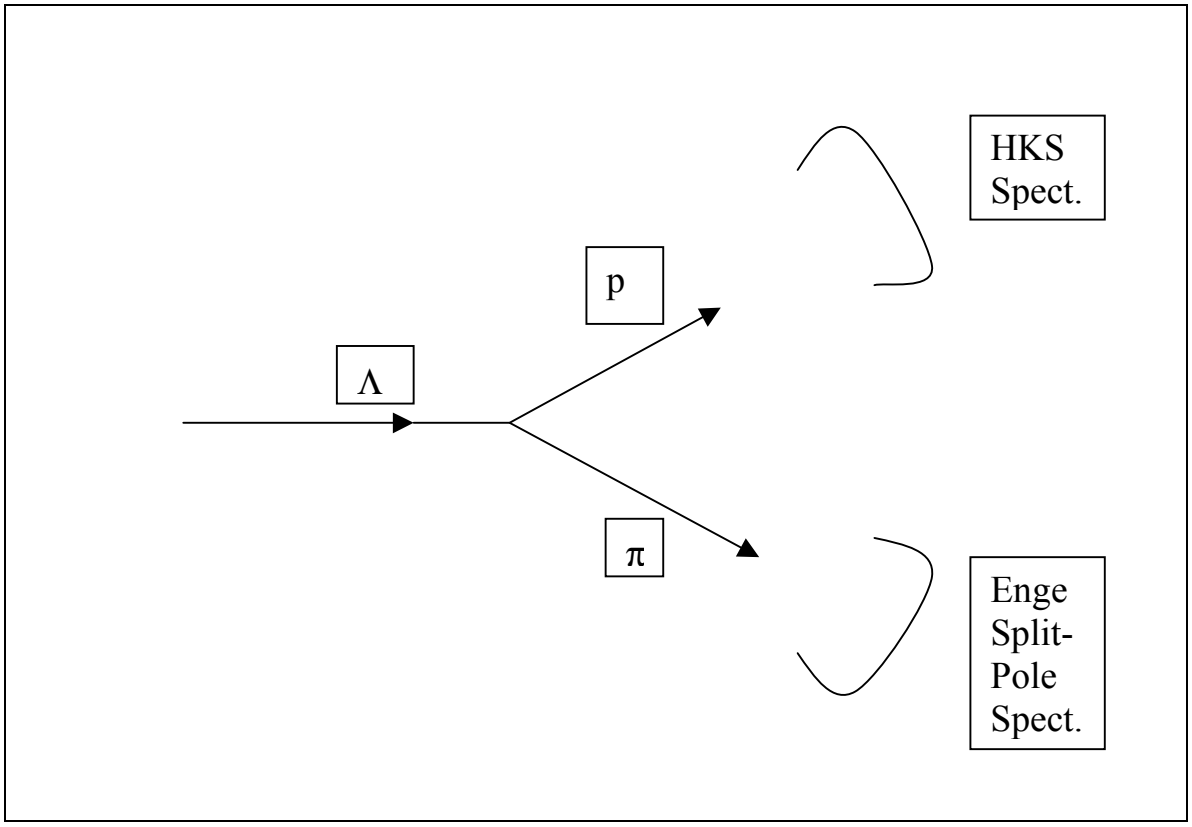

Fig. 2. The weak decay of the Λ hyperon. The proton from the decay will be detected in the High-Resolution Hypernuclear Kaon Spectromter (HKS) while the pion will be detected in the Enge Split-pole Spectrometer. This measurement thus makes use of the existing HKS setup (in the Hypernuclear Spectroscopy Experiment).

In the experiment, a polarized electron beam of 0.94 GeV and 25 microampers current will be used. It is expected that at this beam current, linearly polarized electrons of up to 80% polarization will be achieved. The experiment will use a solid polyethylene (CH_2)

foil for the proton target. CH_2 has a density of approximately 0.94 grams/cc (useful for luminosity calculation). The CH_2 target thickness will be roughly 1 cm. So for an incident electron beam intensity of 25 microampers, the experimental luminosity will be almost 10^{38} $cm^{-2}s^{-1}$. The electroweak production cross sections considered in this LOI can be as high as 10^{-39} cm^2sr^{-1}. For the calculations of the count rate here, we use the conservative value of $3x10^{-40}$ cm^2sr^{-1} to get the estimate of approximately 10 counts per day.

Details of the experimental setup and procedure are given in section III of this Letter of Intent.

Physics Motivation

Determination of weak nuclear form factors

The differential cross section for the reaction (1) may be written as [11]

$$\frac{d\sigma}{d\Omega} = \frac{m_e m_\nu G^2 m_f p_f |M|^2}{(2\pi)^2 E 8 \left| m_i + E - E E_f \cos\theta / p_f \right|} \tag{2}$$

where m_e and m_ν are the electron and neutrino masses, G is the Fermi coupling constant, m_f denotes the final state hyperon with momentum p_f and energy E_f. E is the incident electron energy, m_i is the proton mass, and θ is the angle between the incident electron and the outgoing Λ-hyperon. M is the electroweak matrix element expressed in terms of the weak form factors via the vector and axial-vector weak couplings:

$$M \sim \left\langle \Lambda \left| V_\mu^{\,!}(0) \right| p \right\rangle - \left\langle \Lambda \left| A_\mu^{\,!}(0) \right| p \right\rangle \tag{3}$$

$$\left\langle \Lambda \left| V_\mu^{\,!}(0) \right| p \right\rangle = \bar{u}_f \left[\chi_\mu F_v(q^2) + i \frac{F_M(q^2)\sigma_{\mu\nu} q^\nu}{2m_p} - F_S(q^2) \frac{q_\mu}{2m_p} \right] u_i \tag{4}$$

$$\left\langle \Lambda \left| A_\mu^{\,!}(0) \right| p \right\rangle = \bar{u}_f \left[\chi_\mu \chi_5 F_A(q^2) + i \frac{q_\mu \chi_5 F_P(q^2)}{2m_\pi} + \frac{i F_E(q2) \sigma_{\mu\nu} q^\nu \chi_5}{2m_p} \right] u_i \tag{5}$$

Shown in Fig. 3 is the differential cross section for the reaction (1) versus Λ laboratory angle for several different incident electron energies. The cross section peaks rather sharply at a hyperon lab angle of about 40° for an incident energy of 1 GeV; the cross section is approximately 10^{-39} cm^2/sr there. The experimental proposal here would use an incident electron energy of 940 MeV.

The contribution of the various form factors to the differential cross section is shown in Fig. 4 as a function of the outgoing Λ laboratory angle for an incident electron energy of 4.0 GeV. The dominant contribution comes from the axial-vector form factor F_A over most of the angles, although they all peak at about 50° for this energy. The calculations for a 1.0 GeV incident beam are being made presently.

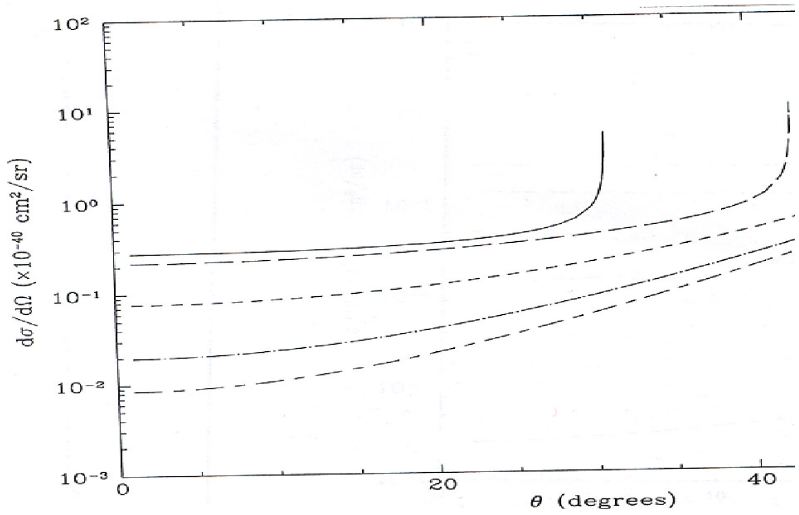

Fig. 3. The laboratory differential cross section for weak production of Λ-hyperons versus the angle that the hyperon makes with the incident beam direction. The cross section is shown for several different incident electron energies from 0.5 to 6.0 GeV. The figure is taken from [11].

Stellar dynamics

The weak process described in this LOI is of major importance in stellar dynamics and supernovae explosions [12]. Weak production of nucleons and hyperons are believed to be a means of removal of internal energy from an expanding shock wave in core collapse during supernovae formation [12]. There are predictions that strange stars, that is stars that have significant s-quark or hyperon dynamics, are more abundant in our universe than neutron stars. The process

$$u + d \leftrightarrow s + u \tag{6}$$

is believed to be the dominant one sustaining these predicted strange stars. The reaction involving the up and strange quark will be studied in the JLAB experiment.

Relation to Drell-Yan-like process to be studied at the Large Hadron Collider

The reaction shown in Fig. 1 is related to the Drell-Yan-like production of W bosons that will be studied at the Large Hadron Collider (LHC). At the LHC, the proton-proton

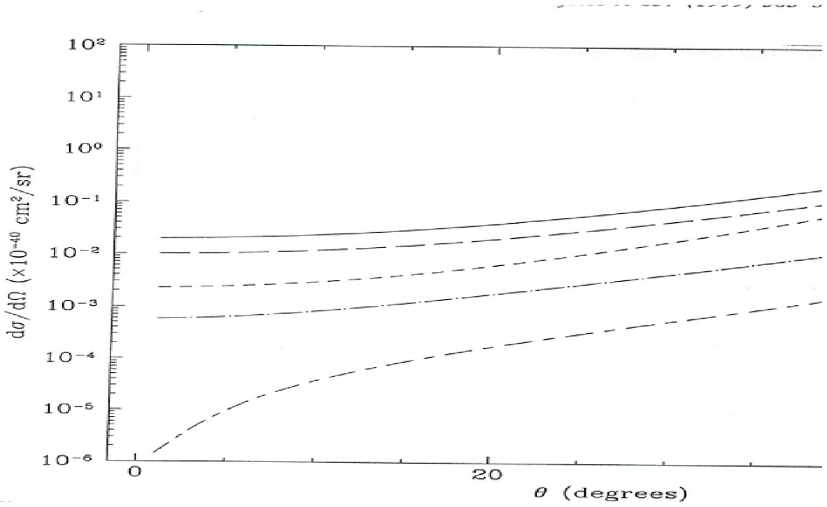

Fig. 4. The contributions from several form factors that contribute to the weak production process versus the angle that the Λ-hyperon makes with the incident beam direction. All of the form factors peak at about 50 degrees for this incident electron energy (4.0 GeV). The figure is taken from [11].

collisions at 14 TeV center of mass energy may be viewed as the scattering of the hadron's constituents. Precision electroweak measurements form one of the most compelling reasons for the construction of the LHC and its detectors. The lowest-order diagram describing the LHC process of interest in this LOI is shown in Fig. 5.

This mechanism of producing W bosons represents one of the cleanest processes with a large cross section at the LHC [13]. The LHC reaction is well suited for a precision measurement of the W boson mass, and it is expected to yield valuable information on the parton structure of the proton. The lowest-order differential cross section for the reaction of Fig. 5 can be related to the CKM matrix element $V_{qq'}$. The JLAB experiment

shown in Fig. 1 can, in principle, provide complimentary information about this electroweak process and therefore information on the CKM matrix element as well.

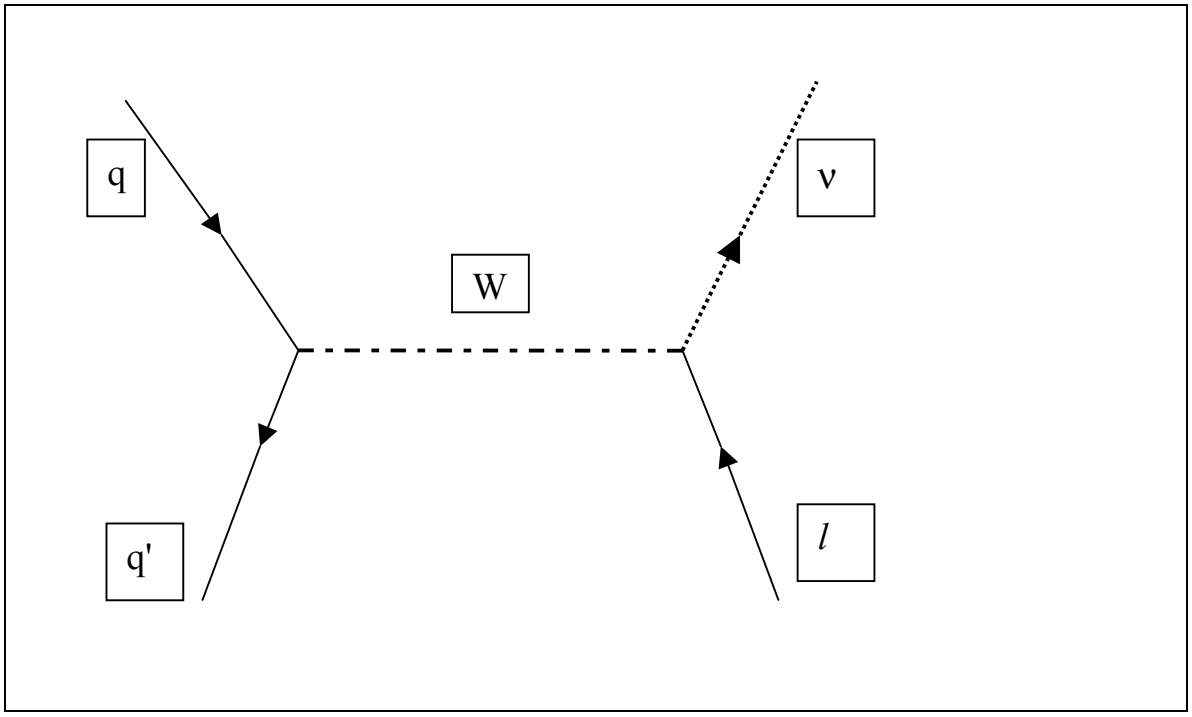

Fig 5. The lowest order Drell-Yan-like diagram for W boson production at the LHC. This process is similar to the reaction to be studied in the JLAB experiment described in this LOI (see Fig. 1).

Experimental Procedure

The experiment will be studied in Hall C using the High Resolution Kaon Spectrometer (HKS) and the Enge Split-pole Spectrometer. The HKS will be used to detect and identify the protons in a modest background of positive pions and a small background of kaons. The collaboration has had extensive experience using the Hall C SOS and Enge to detect electron-kaon coincidences in the past. The detector stack to be used in the HKS is practically identical to the one that was used in the SOS. The detector stack to be used is shown in Fig. 6 below.

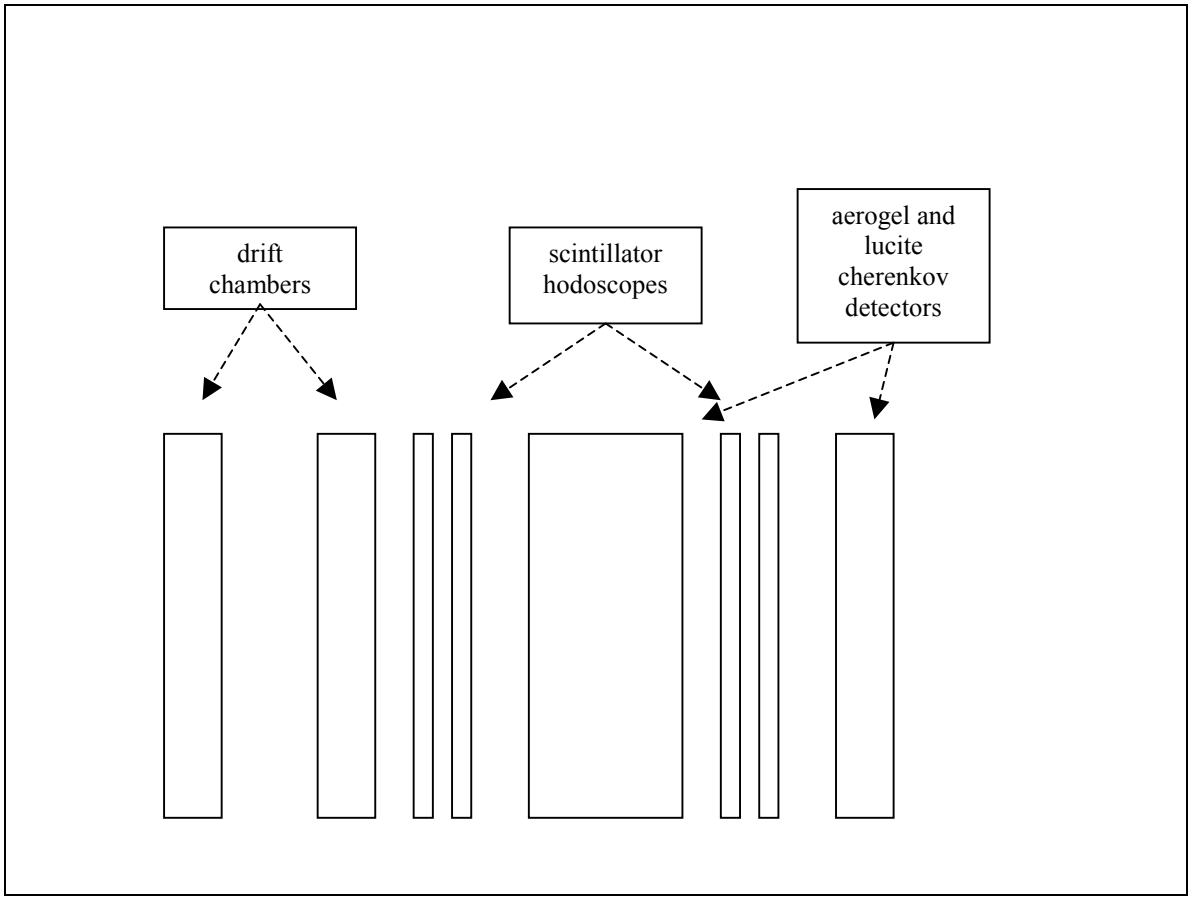

Fig.6. The proposed detector stack for the HKS spectrometer (the hadron arm). This is the same detector stack that was used in the HNSS experiment E89-009 at JLAB. The particles to be detected are incident from the left.

The HKS will have two sets of planar drift chambers for particle trajectory reconstruction. There will be six planes per chamber (XYUVY'X'). The wire chambers used in conjunction with the spectrometer magnets is expected to yield a momentum reconstruction accuracy, $\delta p/p$, of better than $5x10^{-4}$. There will be two sets of scintillator hodoscopes for triggering and fast timing. Each set will contain X and Y hodoscope planes. Previous experience with the SOS scintillator hodoscopes has shown that it is not

unreasonable to expect timing resolutions per plane, δt, of better than 300 ps. For particle identification (pid) the HKS will make use of two types of Cherenkov detectors, a silica aerogel-based diffusion box detector and a total internal reflection lucite counter. A similar system used in the SOS during the HNSS experiment (JLAB Experiment E89-009) achieved pion/kaon separations of better than 300/1 and proton/kaon separation of better than 200/1. These will be more than adequate for the present study.

The Enge Split-pole Spectrometer will be used to detect and identify negative pions in a background of electrons and muons, mainly. The spectrometer is the same that was used in E89-009, but now with a proposed new detector stack shown in Figure 7.

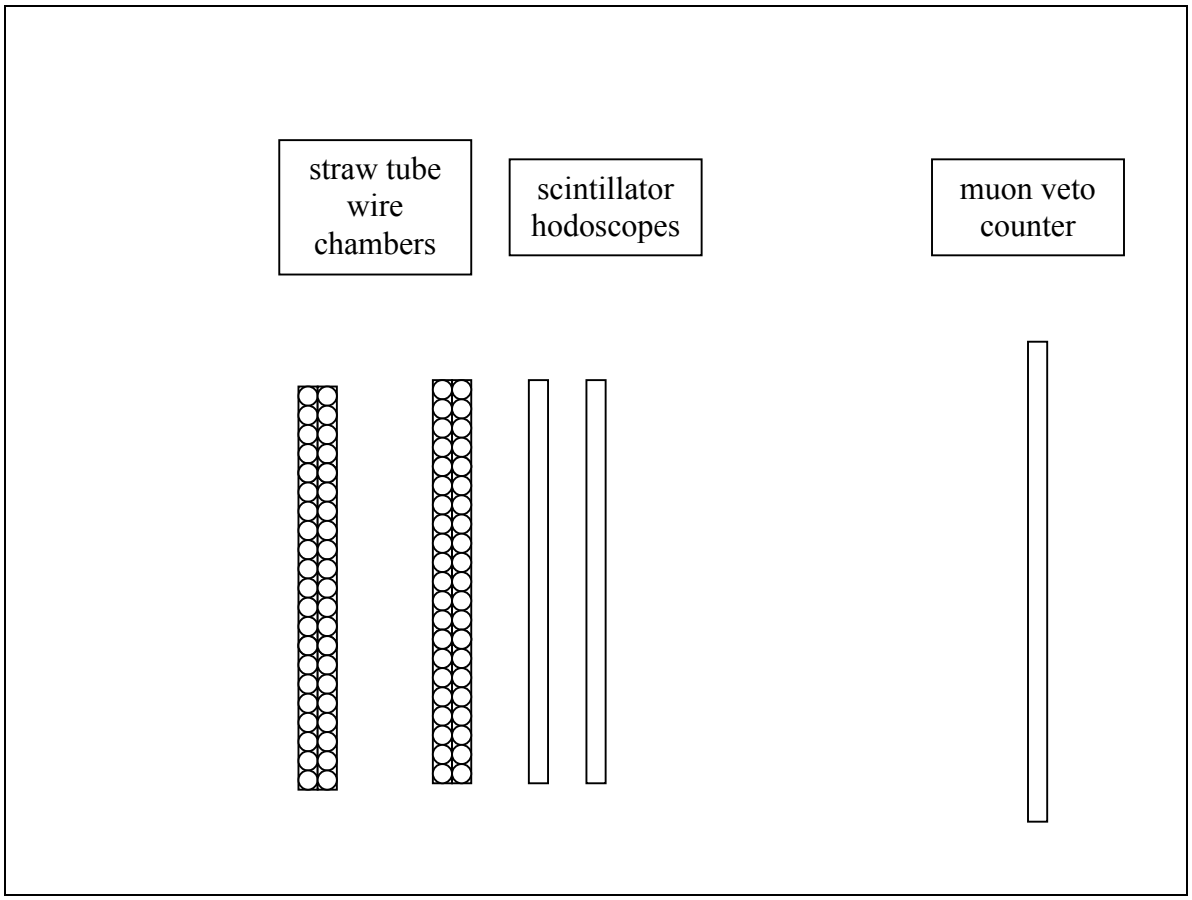

Fig. 7. The proposed detector stack for the Enge Split-pole Spectrometer (the negative hadron arm). This is the same spectrometer that was used in JLAB experiment E89-009, only with a new detector arrangement. The particles to be detected are incident from the left.

There is a strong correlation between the angle and momenta of the emergent proton and pion coming from the hyperon decay. For fixed spectrometer angles (and acceptances) the decay particles' momenta are specified for the reaction under study. Simulations have been done for an incident electron momentum of 940 MeV, and zero degree settings (with respect to the incident electron beam) for both spectrometers. The HKS and Enge

spectrometers will have an angular bite large enough to detect protons of up to four degrees and pions up to 0.5 degrees, respectively, with respect to the incident electron beam. Thus the maximum angle between the proton and pion from the hyperon decay will be about 4.5 degrees (in the laboratory frame). The proton momentum will be approximately 0.87 GeV/c while the pion momentum will be approximately 0.33 GeV/c in order to detect the reaction given in (1).

Previous experience with Jefferson Lab experiments E91-016, E93-018, and E89-009 (all kaon electroproduction experiments) indicate that the coincidence spectrum for the HKS will be that shown in Fig. 8. Displayed in this figure along the vertical axis is the velocity of the positive hadron detected (with respect to the speed of light) versus the coincidence time along the horizontal axis. There are three different particle types detected; positive pions (β~1), kaons (β~0.9), and protons (β~ 0.8).

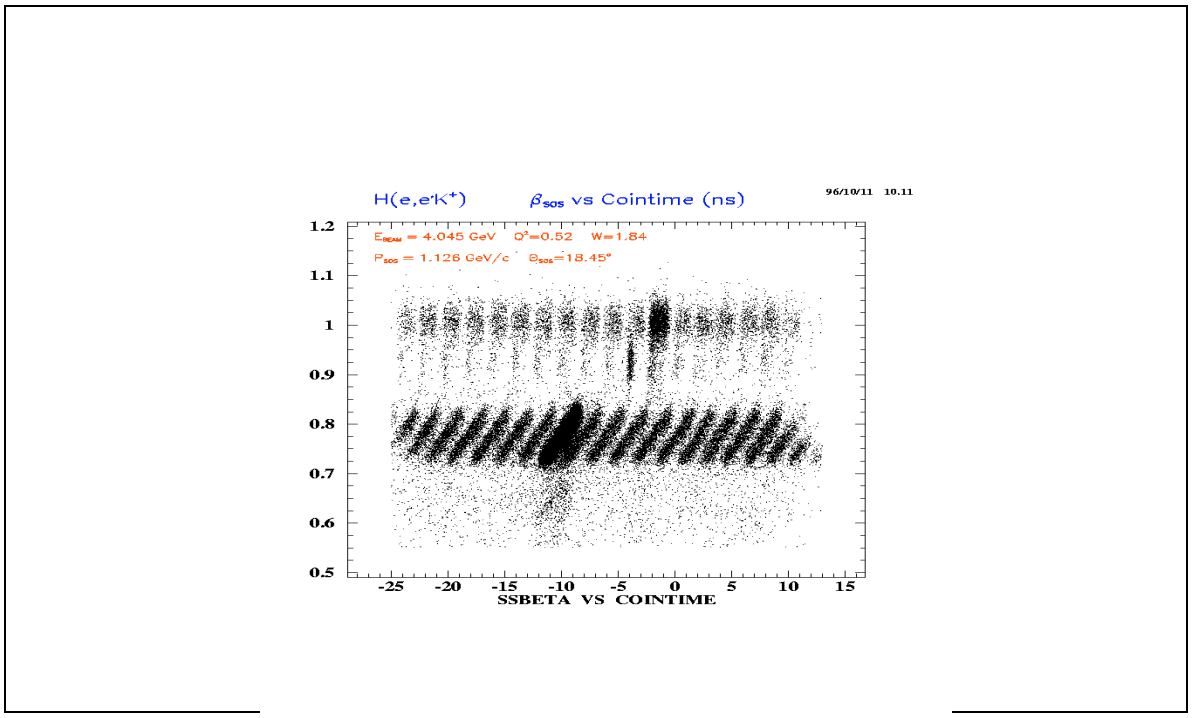

Fig. 8. The coincidence spectrum from Experiment E93-018 at the positive hadron arm spectrometer momentum setting appropriate for studying reaction (1). There are three different types of positive hadrons clearly identified - pions, kaons, and protons. This spectrum is identical to the one expected for the HKS in the coincidenct experiment.

The hodoscope timing will be sufficiently accurate to separate the rf structure of the CEBAF beam. A representative spectrum taken from the Enge Split-pole Spectrometer of E89-009 is shown in Fig 9. This same rf structure is seen along the horizontal axis of Fig. 8. The missing mass spectrum shown in Fig. 10 is generated from the information shown in Figs. 8 and 9. In this case, taken again from Experiment E89-009, a cut was made of the kaons from Fig. 8, and the appropriate srf bucket for electrons from Fig. 9.

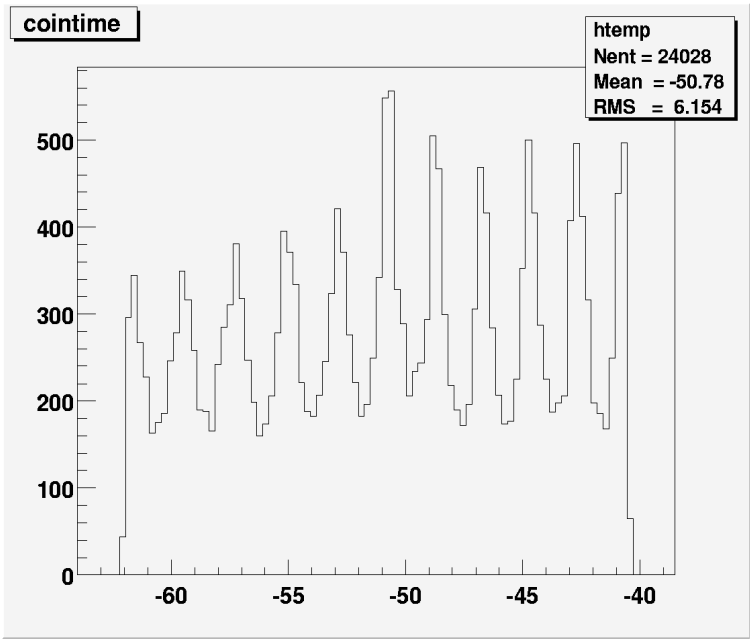

Fig. 9. The rf structure of the CEBAF beam. Timing relative to these beam bursts are used for particle identification.

The peaks corresponding to the Λ and Σ^o hyperons are clearly seen in the missing mass spectrum of Fig. 10. These hyperons coming from the hydrogen in the CH_2 target clearly stand out on top of the broad distribution of randoms events and contributions from the carbon scattering.

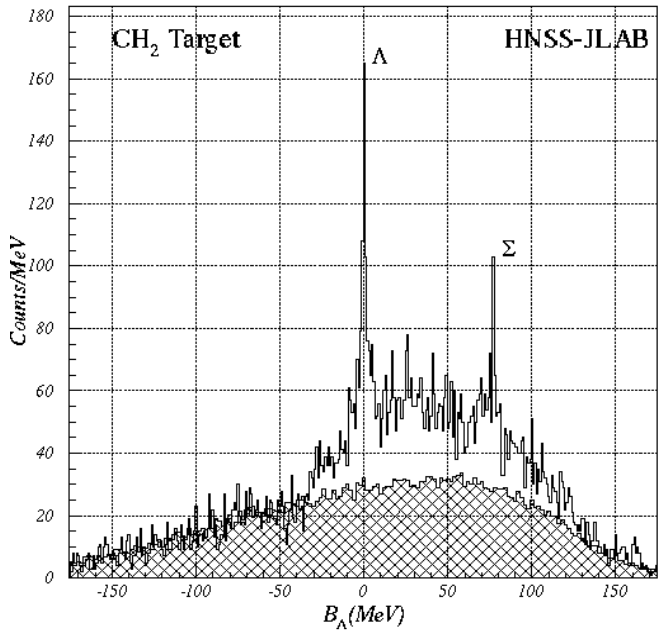

Fig. 10. The missing mass spectrum calculated from the kaons detected in the SOS and the electrons detected in the Enge Split-pole Spectrometer from experiment E89-009. The Λ and Σ^o hyperons from the reaction on the hydrogen in the CH_2 target are clearly identified on top of accidental coincidences, and the background events coming from scattering from carbon. It is expected that the Λ hyperon peak from reactions (1) can be cleanly identified in a similar manner in the proposed experiment.

In Fig. 10, accidental background contributions (including some pion contamination) to the spectrum has been estimated by using eight accidental coincidence time windows surrounding the real coincidence peak and subtracted. The effect of beam energy drift is found to be negligible.

Separating out the carbon contribution to the scattering is expected to be straightforward, based upon prior experience in E89-009. A long carbon run yields the spectrum shown in Fig. 11. The distributions is fitted quite easily as shown. The subtraction of the carbon contribution from the CH_2 target will be done bin-by-bin. For the spectrum shown in Fig. 11, the background includes accidentals and real coincident pions leaking through the cut on particle velocity (β). The accidental coincidence peaks were used for accidentals' analysis.

The percentage of real coincident pion leaking through was analyzed using fits in the beta cut for both real and accidental coincidences. The difference gave the real pion leak-through; accidental pions are naturally included in the accidental background. The pion

selection with (e,e'K+) kinematics gives the histogram shape. The background was fitted by a fourth order polynomials with confidence level of 100%. The Chi-square per number of degrees of freedom, confidence level, and the actual function are shown in the figure.

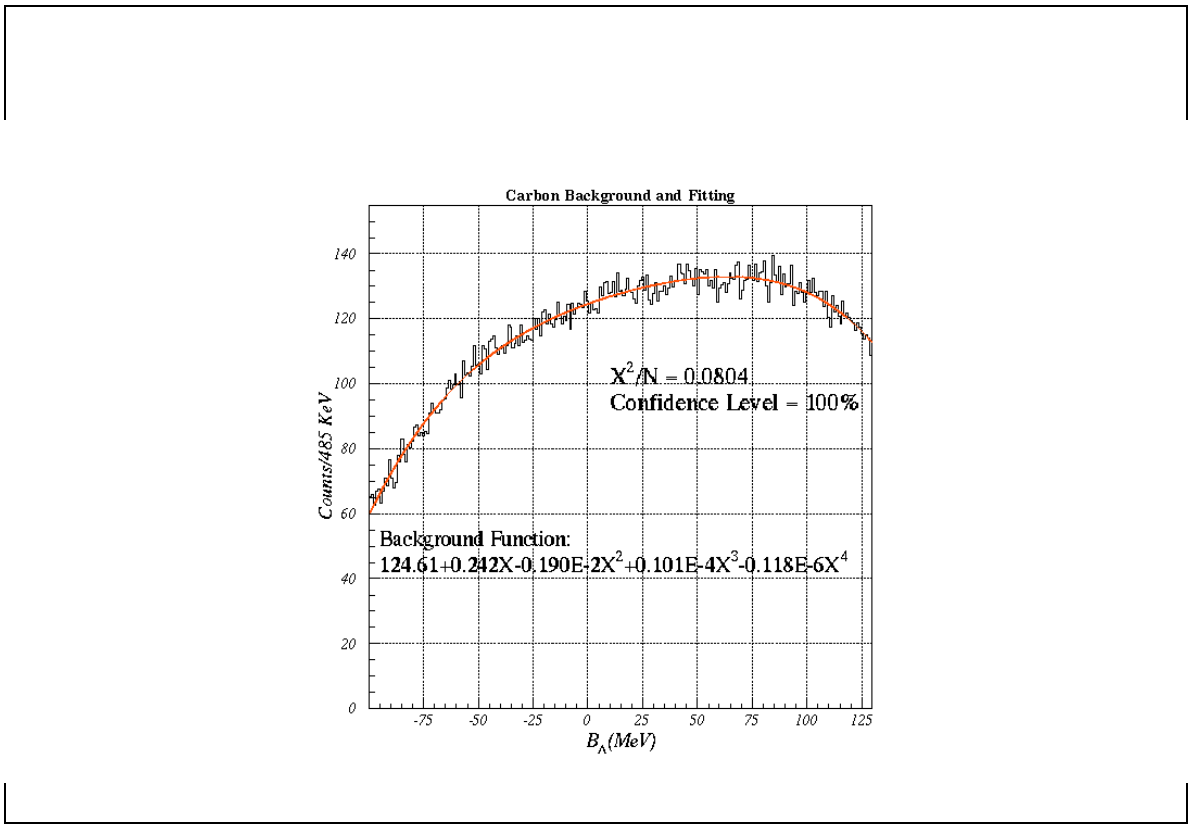

Fig. 11. The analysis of the background coming from scattering on carbon in the CH_2 spectrum.

The experiment proposed in this LOI will use a CH2 target of approximately 1 cm in thickness. The target will be cooled by placing it on a Be backing as shown in Fig. 12. The heat dissipation achieved with this setup will be adequate to handle a 30 μA beam-on-target.

Simulations using the SOS and Enge Split-pole Spectrometer setup in Experiment E89-009 indicates that the measurment proposed here is feasible. Using the energy and momenta of the pion and proton (from the hyperon decay) allows a reconstruction of the missing mass. This simulation, shown in Fig. 13, indicates that the Λ peak at 1.115 GeV will stand out above the background sufficiently to identify it. The simulation using realistic production from a CH_2 target, with real and random pion-proton coincidences. The HNSS system achieved an energy resolution of better than 800 keV in the missing mass spectrum shown in Fig. 10. This is useful in the proposed experiment. The peak

should sit in a very narrow region of the spectrum compared with the backgrounds which are spread out over the entire spectrum as shown in Fig. 13.

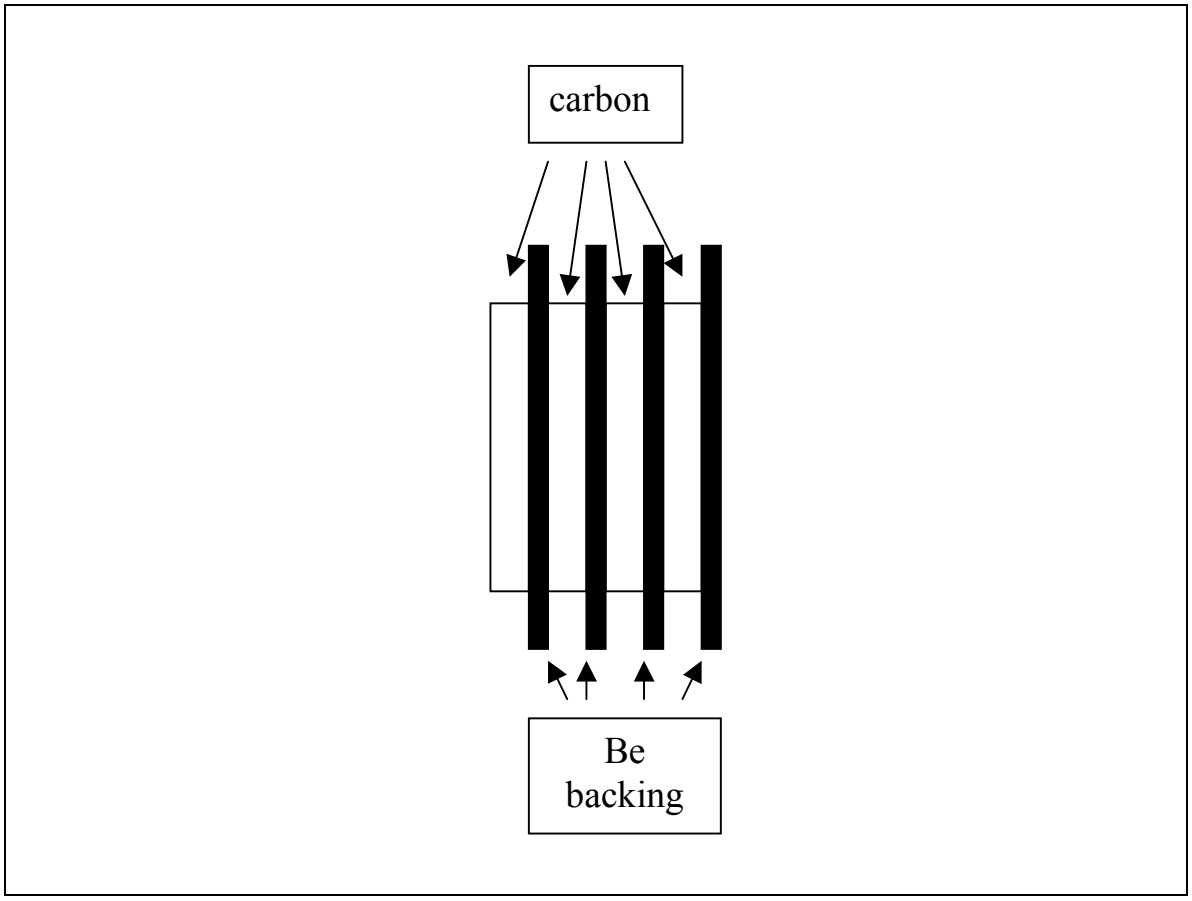

Fig. 12. The proposed CH_2 target for the proposed experiment. The CH_2 foils will be mounted on a Be backing which will provide stability and a path for cooling. The Be will contribute a negligible amount to the coincidence spectrum .

For the simulated spectrum shown in Fig. 13, the SOS was set to a central momentum of 1.1 GeV/c (the SOS has a +/- 20% momentum bite). This allows the protons of roughly 0.87 GeV/c to be easily detected with a cut on particle velocity. This is shown in Fig. 8 where the SOS was at approximately this momentum setting. The Enge Split-pole Spectrometer which will detect the pion has a large momentum bite as shown in Fig. 14. The Enge Split-pole Spectrometer was used to detect the electrons during experiment E89-009 (HNSS Experiment). A good calibration of the spectrometer was obtained for the detection of electrons in the (e,e'K) reaction with the hyperon missing mass calculated as shown in Fig. 10.

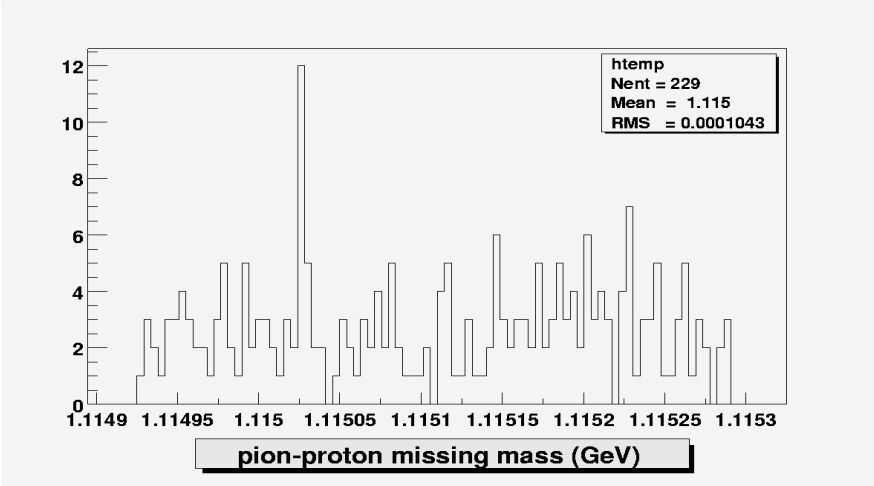

Fig. 13. The missing mass spectrum calculated from the detected pion and proton resulting from the hyperon decay. The peak at 1.115 GeV stands out well enough above background to be clearly identified. This spectrum represents what may be expected in a single day of running.

The weak production experiment proposed here will use straw-tube wire chambers as opposed to silicon strip detectors which were used in the HNSS experiment. Thus, some information on the angle that the detected charged particles make (with respect to a central axis through the detector stack) will be gathered. It is expected that some calibration data using the (e,e'K) reaction on hydrogen will be gathered before this experiment runs. The calibration should be good for the experiment proposed here.

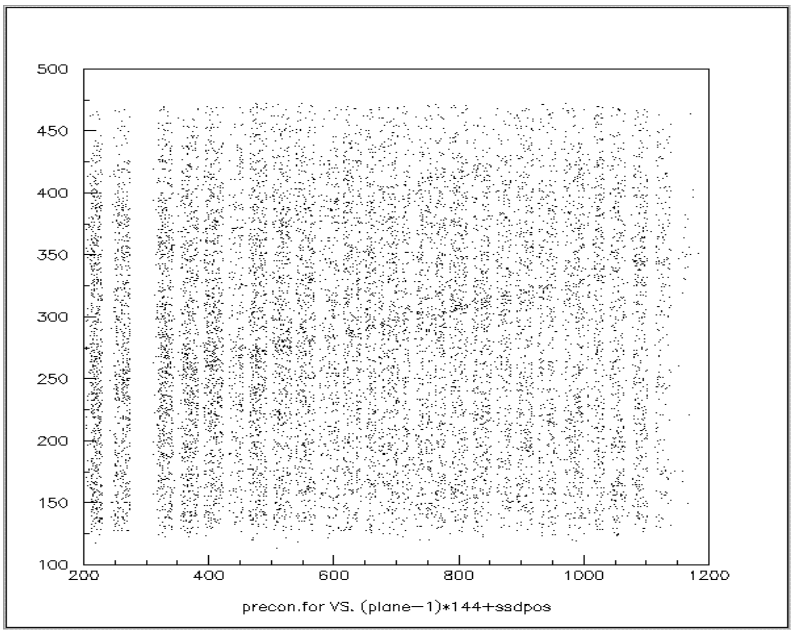

Fig. 14. The momentum of the Enge Split-pole Spectrometer is shown along the vertical axis versus the Silicon Strip Detector channel along the horizontal axis. This calibration was taken during the HNSS Experiment E89-009. The dark band in the center of the spectrum is the reconstructed Λ hyperon from the p(e,e'K)Λ reaction on a CH_2 target. It is expected that a similar calibration spectrum will be acquired before this proposed weak production experiment is run.

Once the hyperon missing mass is reconstructed, the reaction shown in Fig.2 is identified. Then the information from the incident electron beam and target proton may be used to reconstruct the neutrino missing mass. This was simulated, again using a realistic CH_2 target along with real and random coincidences. An unpolarized electron beam of 940 MeV was incident upon the target. Then using equation one the spectrum shon in Fig. 15 was obtained. Note that the neutrino peak stands out above background for the same reason as given for Fig. 13. It is expected that when a polarized electron beam is used, the helicity of the beam along with the fact that the electron neutrino resulting from (1) is left-handed may reduce the background even further. Fig. 15 uses the information from Fig. 13 (same calculations and cuts applied). Again, this represents about one day of running for the experiment conditions in the proposed weak production experiment.

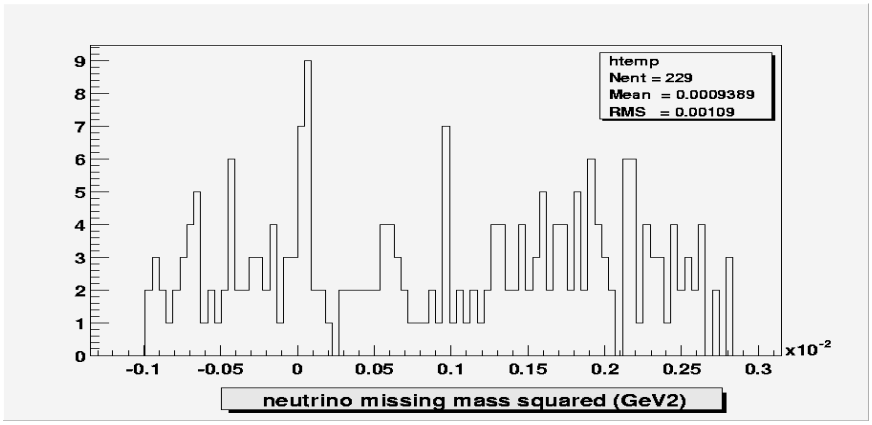

Fig. 15. The missing mass squared from the reaction given in (1). This uses the information from the spectrum of Fig. 13. The neutrino peak stands out above background well enough to be identified. It is expected that the use of a polarized electron beam will be useful in reducing the background even further as explained in the text. This spectrum represents about one day of running for the proposed weak production experiment.

Rates and Beam Time Request

The experiment will use the standard Hall C data acquisition system (CODA) and analyzer appropriate for the HKS experiment already approved. The data rates will be approximately the same in both experiments. Additionally, this experiment will provide valuable calibration data for the approved HKS experiment.

Experience with E89-009 shows that this proposed experiment can expect singles rates in the Enge spectrometer of up to 1 MHz and in the HKS of approximately 800 kHz when a 30 μA incident electron beam is incident upon the 1-cm CH_2 target. The coincidence rate (counts per second) expected is given by

yield = luminosity (cm^{-2} s^{-1}) *x* cross-section (cm^2 sr^{-1}) *x* acceptance (sr) *x* efficiencies.

The luminosity will be approximately 10^{38} cm^{-2} s^{-1} while the cross section used is $3x10^{-40}$ cm^2 sr^{-1}. Note that this is approximately one-third of the maximum cross section expected from the published calculations (see Fig. 3). It is important to note that the particles detected (the pion and proton from the Λ-hyperon decay) are correlated; once one is detected, the other is constrained in kinematics. This is important in calculating the spectrometer acceptances in the coincidence experiment. Only the smaller of the two single arm acceptances needs to be used. Thus an experimental acceptance of 10 msr is used in the calculation. The efficiencies include the following: tracking efficiency in both arms (85%), hyperon decay branching ratio (64%), hodoscope detection efficiency in both arms (95%), computer live-time (95%), and Cherenkov detector efficiency in HKS (90%). Thus a total efficiency for the yield calculation is approximately 0.4. Taken together, the numbers indicate that an integrated yield for coincidences from reaction (1) is approximately 10 counts per day. In a week-long run, approximately 12% statistics will be achieved. This will be the very first time that such a measurement has been made.

An estimate of the accidental (*accid*) to real (*real*) coincidence rate may be obtained (crudely) from

$$\frac{accid}{real} = \frac{R_{HKS} R_{Enge} \tau}{R_{coin}} \frac{1}{df} \qquad (7)$$

where *R* represents the singles rates in the numerator and the expected coincidence rate in the denominator of (7), τ is the resolving time, and the duty factor (*df*) is 1. Using conservative estimates of the HKS proton singles rate (~ 1 kHz), the Enge pion singles rate (~200 Hz) and an offline resolving time of 800 ps yields an accidental to real rate of roughly one to one or better. Note that the accidental coincidences will occupy the entire time window (a flat missing mass spectrum for example), while those real coincidence events will reconstruct the narrow Λ peak in just a few bins; the peak will stick out well above the background in this case. This will be simulated in the full proposal for later submission.

The requested resources needed are summarized in Table 1.

Table 1: Requested Resources

beam energy	0.940 GeV
beam current	25 microamperes
beam polarization	70% (or highest available)
negative hadron spectrometer	Enge Split-pole
positive hadron spectrometer	HKS
Target	CH_2 (solid target, 1-cm thick)
beam time request	7 days

References

[1] G. Niculescu et.al. Phys. Rev. Lett. (1998)

[2] M. Guidal, J.-M. Laget, and M. Vanderhaeghen, Phys. Lett. **B400**, 6 (1997); Nucl. Phy. **A627**, 645 (1997).

[3] T. Mart, C. Bennhold, and C.E. Hyde-Wright, Phys. Rev. C**51**, R1074 (1995).

[4] R.A. Williams, C.R. Ji, and S.R. Cotanch, Phys. Rev. C**46**, 1617 (1992); Phys. Rev. C**43**, 452 (1991).

[5] R. Schumacher, Nucl. Phys **A585,** 63c (1995).

[6] T. Kitagaki et. al., Phys. Rev. D**42**, 1331 (1990); Phys. Rev. D**34**, 2554 (1986).

[7] G.M. Radecky et. al., Phys. Rev. D**25**, 1161 (1982).

[8] P. Allen et. al., Nucl. Phys. B**176**, 269 (1980).

[9] S.J. Barish et. al., Phys. Rev. D**19**, 2521 (1979).

[10] J. Bell et. al., Phys. Rev. Lett. **41**, 1008 (1978); Phys. Rev. Lett. **41**, 1012 (1978).

[11] S.L. Mintz, Nucl. Phys. A**657**, 303 (1999).

[12] See for example, C. L. Fryer, in Strange Quarks in Hadrons, Nuclei, and Nuclear Matter, edited by K. Hicks, World Scientific Publ, 53, (2000).

[13] G. Altarelli and M.L. Mangano, CERN Proc., 2000-004 (2000).